

CEDARVILLE UNIVERSITY

MODIFICATION OF A LATERAL MIMO MODEL FOR USE AS A HYDROFOIL BOAT DESIGN TOOL AND FLIGHT CONTROL SYSTEM WITH THE ADDITION OF LONGITUDINAL CONTROL

AUTHORS

ETHAN BEACHY

Address: 1118 WINDHAVEN CIRCLE APT. H
BROWNSBURG, IN 46112

Phone: 812.604.3361

Email: EABEACHY@CEDARVILLE.EDU

JONATHAN STANHOPE

Address: 5573 COVINGTON MEADOWS CT.
WESTERVILLE, OH 43082

Phone: 614.928.1943

Email: JBSTANHOPE@CEDARVILLE.EDU

ADVISOR

DR. TIMOTHY DEWHURST

Address: 251 NORTH MAIN STREET
CEDARVILLE, OH 45314

Phone: 937.766.7654

Email: DEWHURST@CEDARVILLE.EDU

30 JUNE 2022



Modification of a Lateral MIMO Model for Use as a Hydrofoil Boat Design Tool and Flight Control System with the Addition of Longitudinal Control

Ethan A. Beachy

Cedarville University — Mechanical Engineering
eabeachy@cedarville.edu

Jonathan B. Stanhope

Cedarville University — Mechanical Engineering
jbstanhope@cedarville.edu

A single-track hydrofoil boat is a watercraft with two struts protruding from the centerline of the hull with hydrofoil wings at their lower ends. Such a boat may be steered by turning one or both struts, with the possible assistance of wing-induced-roll. The height and pitch may be controlled using the foils to balance the weight of the boat with hydrodynamic lift. The Cedarville University Solar Boat Team desires to use such a boat to reduce drag and improve race performance. However, such a boat is unstable, motivating work to create an automatic flight control system using multi-input, multi-output state-space control theory and a feedback loop. Previous progress resulted in a model for steering control. This work was modified and extended to allow the use of any valid combination of steering inputs. A height and pitch control model was also developed and the two combined to produce a single flight control system.

Nomenclature

A	State transition matrix	-
B	Control-Input matrix	-
C	Output matrix	-
D	Feed-through matrix	-
K	Compensation matrix	-
$\tilde{\mathbf{N}}$	Precompensation matrix	-
R	Setpoint vector	-
u	Input (command) vector	-
\mathbf{I}_n	Identity matrix, size $n \times n$	-
$\mathbf{0}_{n,m}$	Null matrix, size $n \times m$	-

γ_f	Front strut steering angle	rad
γ_r	Rear strut steering angle	rad
δ_f	Front foil angle of attack	rad
δ_a	Rear foil differential angle of attack	rad
δ_r	Rear foil mean deflection	rad
δ_{rR}	Rear right foil angle of attack	rad
δ_{rL}	Rear left foil angle of attack	rad
\bar{c}	Strut chord	m
h	Flight height of CG	m
h_0	Flight height setpoint	m
m	Boat total mass	kg
ρ	Fluid density	$\text{kg}\cdot\text{m}^{-3}$
p	Body frame roll rate	$\text{deg}\cdot\text{s}^{-1}$
q	Body frame pitch rate	$\text{deg}\cdot\text{s}^{-1}$
r	Body frame yaw rate	$\text{deg}\cdot\text{s}^{-1}$
u	Longitudinal velocity in body frame	$\text{m}\cdot\text{s}^{-1}$
u_0	Design forward velocity	$\text{m}\cdot\text{s}^{-1}$
v	Lateral velocity in body frame	$\text{m}\cdot\text{s}^{-1}$
w	Vertical velocity in body frame	$\text{m}\cdot\text{s}^{-1}$
S	Wing or strut planform area	m^2
α	Angle of attack	rad
θ	Pitch angle	rad
ϕ	Roll angle	rad
ψ	Yaw angle	rad

This is a summary of variables; more parameters and their values may be found in Appendix B.

1 INTRODUCTION & BACKGROUND

The Cedarville University Solar Boat team has successfully raced solar-powered boats for years in the So-

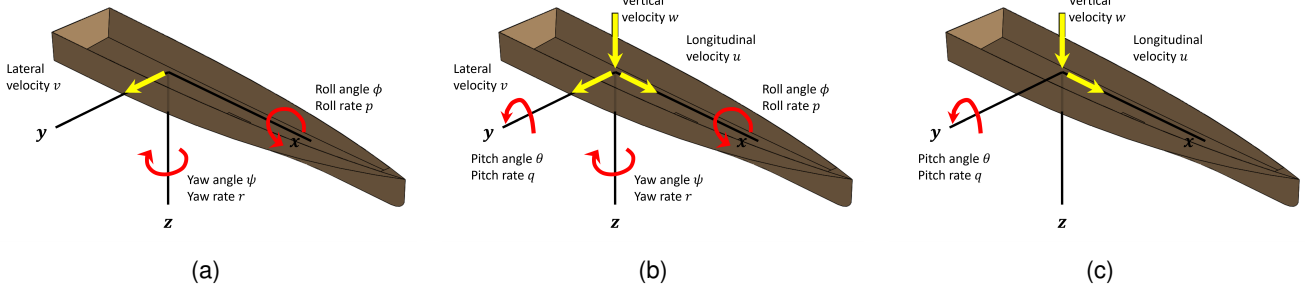


Fig. 1: The 3D coordinates and kinematics (center, shown without struts or foils) may be approximated by separating the lateral (left) and longitudinal (right) models

lar Splash competition in the United States, as well as competing in the European Solar Sport One competition, most recently in 2012. Being competitive in Solar Sport One requires the use of hydrofoils to reduce drag and increase speed.

We have a single-track hydrofoil boat, with two struts on the centerline of the hull that support the foils underwater. The front strut supports a single foil, and the rear strut supports the rear foils, which may be separately articulated. Both struts may also be rotated, resulting in a total of five control surfaces: the front strut, the rear strut, the front foil, the right rear foil and the left rear foil. Instead of considering the right and left rear foils separately, it is helpful consider the rear foil deflections as the superposition of the mean angle of attack (used for height and pitch control) and the difference of each foil from the mean (used for roll control as part of the steering system).

The single-track hydrofoil layout requires the use of a multi-input, multi-output (MIMO) feedback control system. Jason Paulus of the 2021 CU Solar Boat team made significant progress in developing the steering portion of the model [1] to reproduce results published by TU Delft [2]. Paulus mathematically derived the model, then implemented these mathematics as a Simulink simulation. We carried on his work, adapting it to model our boat instead of TU Delft's, and simulating the performance expected from various steering input combinations. We also added longitudinal (height and pitch) control and are working to install and interface with the hardware and electronics required to fly.

Due to the decision to use a different hull design for weight reasons, manufacturing & design setbacks for the struts and actuated steering mechanisms, and resulting delays in installing electronics, we do not currently have an operational boat to use for testing.

1.1 Coordinate System

We use the front-right-down coordinate system widely used in aerospace applications with the x-axis forward motion, the y-axis to the operator's right, and the z-axis down, as shown in Fig. 1.

The orientation of the boat can be described using Euler angles—pitch, roll, and yaw. One potential problem with using Euler angles is gimbal lock. However, we are not concerned about this, as gimbal lock only occurs at pitch angles of $\pm 90^\circ$, in which case gimbal lock is a much lesser issue than the orientation of the boat.

1.2 Assumptions

We made several assumptions to simplify the model and analysis.

- The three-dimensional boat dynamics may be approximated by decoupling lateral (yaw, roll, and sideslip behavior) and longitudinal (forward, vertical and pitch behavior) models. The lateral model controls steering performance and the longitudinal model provides height and pitch control.
- Each model may be described using a linear time-invariant (LTI) state-space representation.
- The models may be linearized about an equilibrium operating point with constant forward speed.
- All control surfaces operate in a region where the lift coefficient is independent of Reynolds number and varies linearly with the angle of attack such that $C_L = C_{L0} + C_{L\alpha} \cdot \alpha$, etc.
- The boat is rigid, symmetric about the xz plane, and has constant mass and mass distribution.
- The control system may ignore air drag on the hull in comparison to hydrodynamic forces.

Testing may prove one or more of these assumptions inaccurate and require the use of a time-variant model.

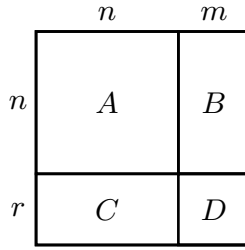


Fig. 2: The sizes of the state-space matrices must match. $ABCD$ must be square to invert when finding the precompensation matrix, so $r = m$. From Paulus [1]

1.3 Instrumentation

To be able to measure the states of the system on the actual boat, we have several sensors: a 9-axis inertial measurement unit (IMU) to measure angular orientation, angular velocity, and acceleration; three height sensors, to find the height at the center of the boat; and a GPS to measure the speed of the boat. These components have yet to be installed.

1.4 Fundamentals of State-Space Control Theory

State-space control theory represents the system dynamics as a system of first-order linear differential equations in matrix form:

$$\dot{\mathbf{x}}(t) = \mathbf{A} \cdot \mathbf{x}(t) + \mathbf{B} \cdot \mathbf{u}(t) \quad (1)$$

$$\mathbf{y}(t) = \mathbf{C} \cdot \mathbf{x}(t) + \mathbf{D} \cdot \mathbf{u}(t) \quad (2)$$

where:

- $\mathbf{x}(t) = [x_1, x_2, \dots, x_n]^T$, the state vector ($n \times 1$),
- $\mathbf{u}(t) = [u_1, u_2, \dots, u_m]^T$, the input vector ($m \times 1$) which here represents the deflection of the control surfaces,
- $\mathbf{y}(t)$ is the output vector ($r \times 1$),
- \mathbf{A} is the state matrix ($n \times n$),
- \mathbf{B} is the input matrix ($n \times m$),
- \mathbf{C} is the output matrix ($r \times n$), and
- \mathbf{D} is the feed-through matrix ($r \times m$).
- n is the number of state variables.
- m is the number of input variables.
- r is the number of output variables (and the number of setpoints the system can track).

The goal is to use the linearized equations to model the system, with the A and B matrices representing the plant, which in our case is the boat dynamics. Linear algebra techniques may then be applied to determine the gain matrices required to stabilize and tune the system. We implemented this using MATLAB and Simulink.

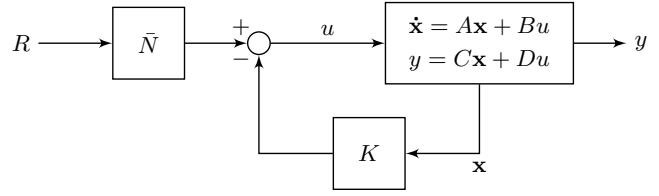


Fig. 3: Block diagram representation of precompensated state-space feedback control loop. From Paulus [1]

These gain matrices are used as part of the control system which we implemented in Simulink. Data from the sensors and the user's selected setpoints fed into these matrices, which are used to calculate the necessary angles of the control surfaces.

The matrix sizes may be seen in Fig. 2. Note that

$$\mathbf{A} = \begin{bmatrix} \frac{\partial \dot{x}_1}{\partial x_1} & \frac{\partial \dot{x}_1}{\partial x_2} & \dots & \frac{\partial \dot{x}_1}{\partial x_n} \\ \frac{\partial \dot{x}_2}{\partial x_1} & \frac{\partial \dot{x}_2}{\partial x_2} & \dots & \frac{\partial \dot{x}_2}{\partial x_n} \\ \vdots & \vdots & \ddots & \vdots \\ \frac{\partial \dot{x}_n}{\partial x_1} & \frac{\partial \dot{x}_n}{\partial x_2} & \dots & \frac{\partial \dot{x}_n}{\partial x_n} \end{bmatrix} \quad (3)$$

and

$$\mathbf{B} = \begin{bmatrix} \frac{\partial \dot{x}_1}{\partial u_1} & \frac{\partial \dot{x}_1}{\partial u_2} & \dots & \frac{\partial \dot{x}_1}{\partial u_m} \\ \frac{\partial \dot{x}_2}{\partial u_1} & \frac{\partial \dot{x}_2}{\partial u_2} & \dots & \frac{\partial \dot{x}_2}{\partial u_m} \\ \vdots & \vdots & \ddots & \vdots \\ \frac{\partial \dot{x}_n}{\partial u_1} & \frac{\partial \dot{x}_n}{\partial u_2} & \dots & \frac{\partial \dot{x}_n}{\partial u_m} \end{bmatrix} \quad (4)$$

For the sake of simulation, let $\mathbf{C} = \mathbf{I}_n$ and $\mathbf{D} = \mathbf{0}_{r,m}$ to display all state variables; that is, $\mathbf{y}(t) = \mathbf{x}$. Next we stabilize the system using feedback and pole placement techniques to move the system poles from the eigenvalues of the \mathbf{A} -matrix to the eigenvalues of $\mathbf{A} - \mathbf{BK}$. The MATLAB `place()` function will automatically compute the required compensation matrix \mathbf{K} based on the dimensions of \mathbf{B} and specified pole locations. These poles must be in the left half of the complex plane for stability; placing the poles further left results in faster convergence but requires larger control forces, which may cause instability when physical limitations like the control surface range of motion and response time are considered. Increasing the imaginary component of the dominant (rightmost) pair of complex poles decreases damping.

The precompensation matrix $\tilde{\mathbf{N}}$ is required to cause the system performance with feedback to converge to

the desired state setpoint vector R . This may be computed using the formula

$$\bar{\mathbf{N}} = [\mathbf{K} \quad \mathbf{I}_m] \begin{bmatrix} \mathbf{A} & \mathbf{B} \\ \mathbf{C} & \mathbf{D} \end{bmatrix}^{-1} \begin{bmatrix} \mathbf{0}_{n,r} \\ \mathbf{I}_r \end{bmatrix} \quad (5)$$

The state-space feedback control loop is shown in Fig. 3. Note that the system determines the control inputs that make up the u -vector by comparing the pre-compensated setpoint vector with the compensated state vector:

$$\mathbf{u} = \bar{\mathbf{N}} \cdot \mathbf{R} - \mathbf{K} \cdot \mathbf{x} \quad (6)$$

2 MODIFICATION OF THE LATERAL MODEL AND USE AS A DESIGN TOOL

2.1 Reasoning

Paulus derived the fully combined steering model for a single-track hydrofoil boat with front and rear strut rotation and rear foil differential (“wingeron”) articulation [1]—that is, the state-space representation for the steering response of the boat when using all three control surfaces. However, we are not obligated to use all available control surfaces, and doing so may not be optimal. If one or more control surfaces could be fixed in place without significant loss of performance this would simplify manufacture, reduce expense, and conserve power for the drivetrain.

The first step was to update Paulus’ model to account for the two struts having different lengths and lift coefficients as shown in Appendix A and to update the simulation’s parameters to be accurate for our boat, as shown in Appendix B. Previously, the model assumed each strut was the same, which is not accurate for our boat, and the model used the parameters for TU Delft’s boat.

Simulating each combination of steering inputs then allowed comparison of steering performance to determine which steering method to pursue. There were six potentially viable combinations out of eight possible: front strut steering, rear strut steering, front strut and wingeron steering, front and rear strut steering, rear strut and wingeron steering, or front and rear struts and wingeron steering (fully combined). The no-input case and wingeron-only control are not viable.

We created MATLAB and Simulink files to simulate the fully combined steering system. The MATLAB script created the state space matrices and performed pole placement to stabilize the system as described by

Paulus, p. 11 [1]. The Simulink model then used these matrices and sample input to plot the boat’s dynamic response. We added the ability to use the same two files to simulate any steering combination.

2.2 Design Methodology

Paulus used the sideslip velocity v , roll angle ϕ , roll rate p , and yaw rate r as the lateral state variables; that is,

$$\mathbf{x}_{\text{lat}}(t) = \begin{bmatrix} v \\ \phi \\ p \\ r \end{bmatrix}. \quad (7)$$

He also showed that the lateral model is controllable. His steering response term for the MIMO model may be expressed in the form

$$\mathbf{B}_{\text{lat}} \cdot \mathbf{u}_{\text{lat}} = \begin{bmatrix} \frac{\partial \dot{v}}{\partial \gamma_f} & \frac{\partial \dot{v}}{\partial \gamma_r} & \frac{\partial \dot{v}}{\partial \delta_a} \\ \frac{\partial \dot{\phi}}{\partial \gamma_f} & \frac{\partial \dot{\phi}}{\partial \gamma_r} & \frac{\partial \dot{\phi}}{\partial \delta_a} \\ \frac{\partial \dot{p}}{\partial \gamma_f} & \frac{\partial \dot{p}}{\partial \gamma_r} & \frac{\partial \dot{p}}{\partial \delta_a} \\ \frac{\partial \dot{r}}{\partial \gamma_f} & \frac{\partial \dot{r}}{\partial \gamma_r} & \frac{\partial \dot{r}}{\partial \delta_a} \end{bmatrix} \cdot \begin{bmatrix} \gamma_f \\ \gamma_r \\ \delta_a \end{bmatrix} \quad (8)$$

where γ_f is the input deflection of the front strut, γ_r is the rear strut deflection, and δ_a is the deflection of each rear foil from the mean position.

The first column of the input matrix represents the steering response to input from rotating the rear strut, the second column that from the rear strut, and the third the effect of using differential rear foil articulation to assist with roll.

Using some but not all steering combinations requires performing pole placement in a restricted setting otherwise instability results. For example, to model front and rear steering, ignore the third input δ_a by passing

$$\mathbf{B}_{\text{place}} = \begin{bmatrix} \frac{\partial \dot{v}}{\partial \gamma_f} & \frac{\partial \dot{v}}{\partial \gamma_r} & 0 \\ \frac{\partial \dot{\phi}}{\partial \gamma_f} & \frac{\partial \dot{\phi}}{\partial \gamma_r} & 0 \\ \frac{\partial \dot{p}}{\partial \gamma_f} & \frac{\partial \dot{p}}{\partial \gamma_r} & 0 \\ \frac{\partial \dot{r}}{\partial \gamma_f} & \frac{\partial \dot{r}}{\partial \gamma_r} & 0 \end{bmatrix} \quad (9)$$

to the `place()` command. The row(s) of the \mathbf{K} matrix corresponding to the unused input(s) will then be only

zeros. In this example that means

$$\mathbf{K}_{\text{lat}} = \begin{bmatrix} K_{1,1} & K_{1,2} & K_{1,3} & K_{1,4} \\ K_{2,1} & K_{2,2} & K_{2,3} & K_{2,4} \\ 0 & 0 & 0 & 0 \end{bmatrix} \quad (10)$$

However, it is slightly less easy to obtain the precompensation matrix $\bar{\mathbf{N}}$, as passing the modified \mathbf{B} -matrix with the column of zeros may make the \mathbf{ABCD} matrix in Equation 5 (reprinted here) singular and therefore non-invertible.

$$\bar{\mathbf{N}}_{\text{place}} = [\mathbf{K}_{\text{lat}} \quad \mathbf{I}_m] \begin{bmatrix} \mathbf{A} & \mathbf{B}_{\text{place}} \\ \mathbf{C}_{\text{place}} & \mathbf{D}_{\text{place}} \end{bmatrix}^{-1} \begin{bmatrix} \mathbf{0}_{n,r} \\ \mathbf{I}_r \end{bmatrix} \quad (5)$$

Instead, only the nonzero columns of \mathbf{B} and rows of \mathbf{K} are used at this step. Inspection of this formula points to another issue. The number of setpoints any control system may track must be less than or equal to the number of possible control surfaces. A modified version of the \mathbf{C} -matrix must be used to “tell” the system which variables to control, as described by Paulus [1]. We would like to track three setpoints: the yaw rate command from the driver, the roll angle command calculated from the yaw rate command to keep sideslip to zero (so gravity provides the centripetal force for a constant turn radius), and sideslip equal to zero. However, using only two of the three control surfaces means the control system may only track two setpoints (yaw rate and either roll or sideslip), and one control surface means tracking only the yaw rate. This keeps \mathbf{ABCD} square, which is required to invert. In this example with front and rear strut steering, controlling sideslip seems to give better roll performance than vice versa. This requires

$$\mathbf{C}_{\text{place}} = \begin{bmatrix} 1 & 0 & 0 & 0 \\ 0 & 0 & 0 & 1 \end{bmatrix} \quad (11)$$

In this example, evaluating Equation (5) produces a 2x2 matrix:

$$\bar{\mathbf{N}}_{\text{place}} = \begin{bmatrix} N_{\text{place}1,1} & N_{\text{place}1,2} \\ N_{\text{place}2,1} & N_{\text{place}2,2} \end{bmatrix} \quad (12)$$

These values must be populated within the 3x3 matrix that the Simulink file used to test the model expects to find in the base workspace. Since δ_a is unused and is

the third element of

$$\mathbf{u}_{\text{lat}} = \begin{bmatrix} \gamma_f \\ \gamma_r \\ \delta_a \end{bmatrix} \quad (13)$$

the third row of $\bar{\mathbf{N}}$ should be zero. The second column should also be zeros because we are not tracking the roll setpoint in the setpoint vector:

$$\mathbf{R} = \begin{bmatrix} v_{\text{set}} \\ \phi_{\text{set}} \\ r_{\text{set}} \end{bmatrix} \quad (14)$$

The elements from the reduced precompensation matrix are placed into the matrix to pass to the Simulink model:

$$\bar{\mathbf{N}}_{\text{lat}} = \begin{bmatrix} N_{\text{place}1,1} & 0 & N_{\text{place}1,2} \\ N_{\text{place}2,1} & 0 & N_{\text{place}2,2} \\ 0 & 0 & 0 \end{bmatrix} \quad (15)$$

The main concept behind the math is that by ignoring unused control inputs we artificially reduce the number of inputs to find the required scaling parameters and populate them into the appropriate positions within the full-scale matrices. Following the same procedure for each viable steering combination means they may all be tested using a single MATLAB script and Simulink model. The MATLAB script contains a string variable to code for the desired steering combination and performs the corresponding pole-placement; the Simulink model then uses them to model the boat’s expected steering performance. This serves a very useful role as a design tool to determine which steering method best meets design objectives like power consumption, steering performance, and hardware requirements.

We also extended Paulus’ work by adding rate limiters and saturation blocks to the input signals to model the boat’s range of motion and response rate limitations. The expected range of motion for the front strut is $\pm 10^\circ$, $\pm 6^\circ$ for the rear strut, and $\pm 6^\circ$ for each rear foil from the mean angle of attack. The foils are expected to have a maximum angular velocity of $\pm 25^\circ/\text{s}$ and the struts about $\pm 40^\circ/\text{s}$. His final model did not function within these limitations; he stated only that instability resulted when he added saturation blocks [1]. Updating the pole placement and adding a rate limit on the yaw rate setpoint solved this problem. He placed the poles

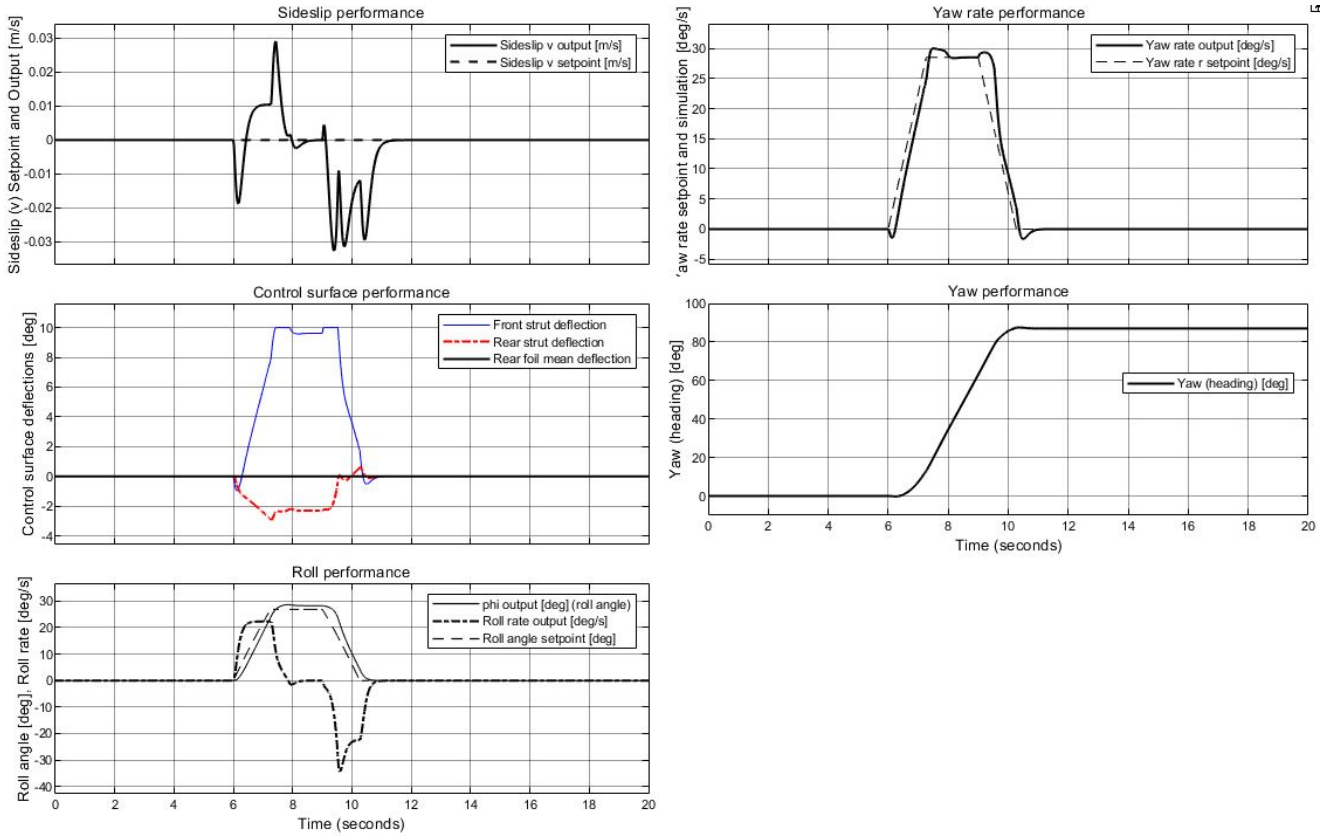


Fig. 4: A diagram showing the predicted response of the lateral control system to a given yaw command using front and rear strut steering. As yaw, roll, and sideslip each track the setpoints well, front and rear strut steering gives good performance without using wingeron-assisted roll control

at $-8 \pm 5i$, -34 , and -3400 for rapid convergence. We found that the last two were so far left that the system demanded displacements and movement rates that exceeded the physical capability of the control surfaces. Also, if the yaw rate setpoint changed too quickly (as with a step input), the boat could not respond quickly enough. Moving the poles to $-10 \pm 1.25i$, -8 , and -14 and limiting the yaw angular acceleration to $22.5^\circ/s^2$ significantly improved stability while achieving sufficiently rapid settling time to track steering setpoints.

2.3 Testing and Evaluation

The ability to simulate each case was important for deciding whether to pursue actuated steering in one or both struts. We used a yaw rate setpoint signal we believe represents the steering input a driver is likely to provide, shown in Fig. 5. This signal is scaled by a gain in the model to represent the desired turn rate. The area under this curve is 3° . Since the gain has units of $^\circ/s$ and the time axis is in seconds, this integral means that the final heading should be three times the gain, e.g. a gain of $20^\circ/s$ should result in a 60° turn.

The simulation helps provide understanding of the

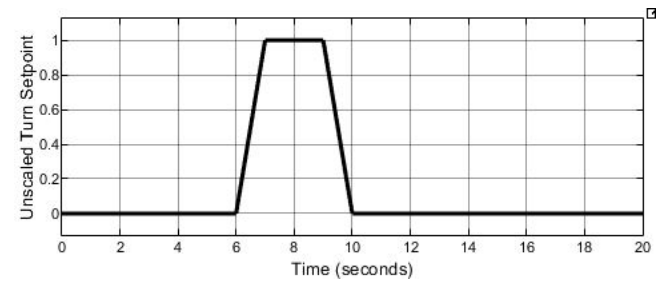
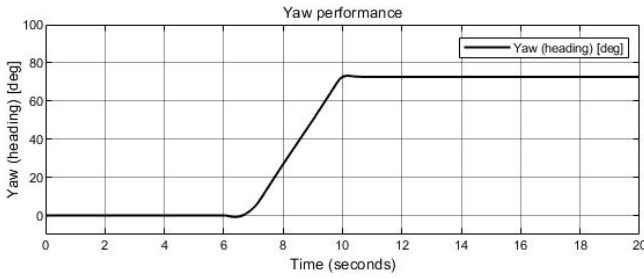
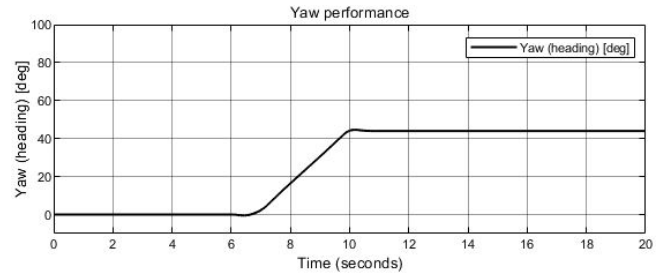


Fig. 5: The yaw rate command signal used for testing and evaluation consists of a one-second ramp to the desired turn rate (dictated by a scale factor), held for two seconds, and a ramp down to return to straight motion at the new heading.

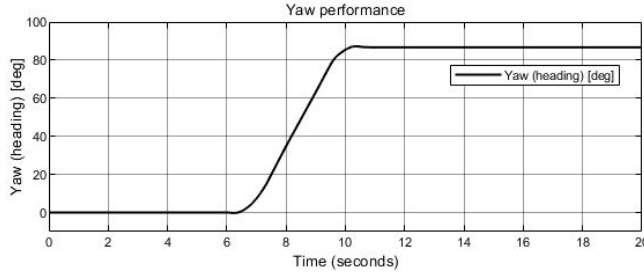
dynamic response that contributes to a tight turn. The example of front & rear strut steering with the maximum stable commanded yaw rate of $28.4^\circ/s$ is shown in Fig. 4. The first thing to note is that the front foil saturates during parts of the turn (the solid blue curve seen in the second window on the left) at 10° of deflection, but the boat remains stable. As expected, the rear foil deflects in the opposite direction from the front strut and the differential deflection remains zero since



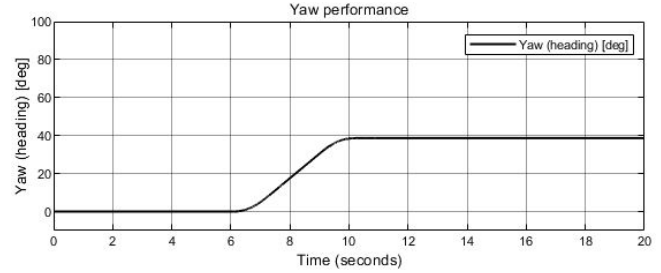
(a) Front steering, yaw rate gain of $23.2^\circ/\text{s}$



(b) Rear steering, yaw rate gain of $14.1^\circ/\text{s}$



(c) Front & rear steering, yaw rate gain of $28.5^\circ/\text{s}$



(d) Fully combined steering, yaw rate gain of $12.9^\circ/\text{s}$

Fig. 6: Front and rear strut steering allows for the highest yaw (turn) rate. Saturation causes instability in all combinations which include wingeron roll assist at lower yaw rates than those which do not.

it is unused in this steering combination. Sideslip—plotted on a much smaller scale—and yaw rate track their setpoints well and the resulting (uncontrolled) roll angle also remains close to its ideal value and never exceeds its max allowable value of 30° . The roll indicates that the boat banks into the turn due to the initial slight counter-steer from the front strut, analogous to turning a bicycle. This is required to keep sideslip low. A similar motion is observed to return to vertical when ending the turn. The distortion in the roll rate, sideslip, and yaw rate curves at about $t = 10$ s is due to the saturation of the front strut, which prevents it from assisting in returning to vertical; the rear strut then does so.

We found the best steering performance of each viable steering method by increasing the commanded turn rate until the system went unstable. The turn performance curves are shown in Fig. 6. The front strut & wingeron control and rear strut & wingeron control are not shown because these models showed unstable behavior at very low turn rates due to saturation of the wingerons. The fully combined model suffered the same issue, though less severely. The highest turn rate is given by front and rear strut steering, which can take a 90° turn in about four seconds. At the design speed of 10 m/s this corresponds to a 20 m turn radius.

However, fully combined steering gave slightly better performance when using a sine-ramped input signal as done by Paulus. This means that the operator is a contributing factor to which model proves most suc-

cessful, especially when the ability to shift weight is taken into consideration. Physical testing is required to make the final determination.

It should also be noted that the problem with wingeron control being unstable could be solved using time-variant state-space control theory and updating the compensation matrices when saturation occurred to the next model which does not use that control surface. This would also require a way to determine when to switch back when the original model would no longer saturate, likely a parallel simulation. We believe that it is unnecessary to pursue the extra complexity unless testing proves it is needed after all hardware components are installed.

Finally, front & rear steering still requires that all control surfaces have actuated position control. No additional hardware will be required if testing reveals that another model gives better performance or that a time-variant model is needed, as these changes occur in the software. Actuated control of all control surfaces keeps control options open, thereby maintaining flexibility.

3 DERIVATION OF LONGITUDINAL MODEL FOR HEIGHT AND PITCH CONTROL

3.1 Reasoning

The boat speed (x -velocity), pitch angle θ , and flight height h belong to the longitudinal model. Forward speed is controlled separately by the operator via the throttle and drivetrain. That means the flight con-

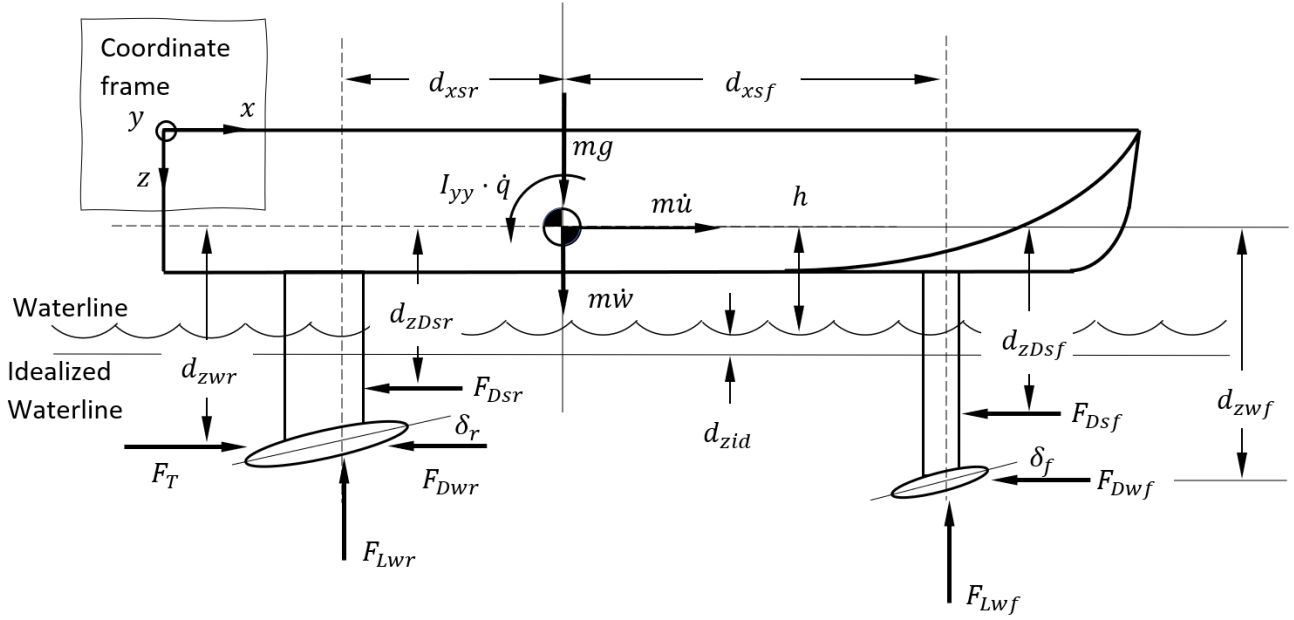


Fig. 7: An accurate and complete free body diagram is essential to correctly apply Newton's Second Law to the longitudinal model. Parameter values may be found in Appendix B.

control system should maintain height and pitch for steady level flight. Therefore h and θ must be state variables in the longitudinal model. With the approximation of decoupled lateral and longitudinal systems, Newton's laws may be applied since the longitudinal model lies completely in the xz -plane. Since Newton's laws require the second derivatives of height and pitch, the first derivatives of height and pitch (w and q respectively) must also be state variables. We organized them in the longitudinal state vector as

$$\mathbf{x}_{\text{long}}(t) = \begin{bmatrix} \theta \\ q \\ h \\ w \end{bmatrix}. \quad (16)$$

The longitudinal model must control two setpoints and therefore requires two control surfaces: the front foil angle of attack δ_f and the mean angle of attack δ_r of the two rear foils. This means that the input vector will be

$$\mathbf{u}_{\text{long}} = \begin{bmatrix} \delta_f \\ \delta_r \end{bmatrix} \quad (17)$$

3.2 Design Methodology

Deriving the equations is the first step toward developing the feedback control loop. The free body diagram for the longitudinal model is shown in Fig. 7.

Because the height measured by the sensors will contain noise due to waves and other surface disturbances, it is desirable that the longitudinal model respond slowly enough to act as a low-pass filter while also fast enough to maintain steady flight. We estimate that a settling time of 1.5–2 seconds is appropriate.

Subscripts describe the forces F and distances d :

- x - "x-direction,"
- z - "z-direction,"
- L - "lift,"
- D - "drag,"
- T - "thrust,"
- s - "strut,"
- w - "wing,"
- h - "hull,"
- f - "front," and
- r - "rear"

so $F_{D,s,f}$ means the drag force on the front strut, etc.

We followed TU Delft in using an offset d_{zid} between the real waterline and an ideal waterline used as to calculate the hydrodynamic forces [2]. We also made several additional simplifying assumptions during the derivation:

- The pitch angle remains small enough to use the small angle approximations $\sin(\theta) \approx \theta$ and $\cos(\theta) \approx 1$

$\cos(\theta) = 1$. This should be valid since the maximum angle possible (with the stern in the water and bow at flight height) is about 5° .

- The center of pressure of the front strut and foil is coincident in the x-direction and occurs at the quarter-chord point.
- Likewise, the center of pressure of the rear strut and foils are coincident in the x-direction and occurs at the quarter-chord point.
- The thrust from the propellers is collinear with the rear foil drag force.

Two of the state equations are trivial to derive. Since the pitch rate is the derivative of the pitch angle,

$$\dot{\theta} = q = [0 \ 1 \ 0 \ 0] \cdot \begin{bmatrix} \theta \\ q \\ h \\ w \end{bmatrix} + [0 \ 0] \cdot \begin{bmatrix} \delta_f \\ \delta_r \end{bmatrix} \quad (18)$$

This means the first row of the A-matrix is $[0, 1, 0, 0]$ and the first row of the B-matrix (which must be 4×2) is $[0, 0]$.

Similarly, the drop velocity is equal to the negative derivative of the height above the water (since the positive z-direction is down).

$$\dot{h} = -w = [0 \ 0 \ 0 \ -1] \cdot \begin{bmatrix} \theta \\ q \\ h \\ w \end{bmatrix} + [0 \ 0] \cdot \begin{bmatrix} \delta_f \\ \delta_r \end{bmatrix} \quad (19)$$

This means the third row of the A-matrix is $[0, 0, 0, -1]$ and the third row of the B-matrix (which must be 4×2) is $[0, 0]$.

The other two rows are obtained by summing forces in the z (vertical) direction and moments about the center of gravity and taking partial derivatives with respect to each state variable and control input to linearize. Using the notation that $Z_{\delta_f} = \frac{\partial \Sigma F_z}{\partial \delta_f}$, $M_\theta = \frac{\partial \Sigma M_x}{\partial \theta}$, etc., the state and input matrices may be written in terms of stability derivatives as:

$$\mathbf{A} = \begin{bmatrix} 0 & 1 & 0 & 0 \\ M_\theta & M_q & M_h & M_w \\ 0 & 0 & 0 & -1 \\ Z_\theta & Z_q & Z_h & Z_w \end{bmatrix} \quad (20)$$

and

$$\mathbf{B} = \begin{bmatrix} 0 & 0 \\ M_{\delta_f} & M_{\delta_r} \\ 0 & 0 \\ Z_{\delta_f} & Z_{\delta_r} \end{bmatrix} \quad (21)$$

After taking partial derivatives it can be shown that:

$$M_q = M_w = 0 \quad (22)$$

and

$$Z_\theta = Z_q = Z_h = Z_w = 0 \quad (23)$$

that is, the vertical acceleration is independent of pitch, pitch rate, height, and drop velocity and therefore only influenced by the lift generated from the foils, which is proportional to the angle of attack.

The remaining stability derivatives are found to be:

$$M_\theta = \frac{\rho u_0^2}{2I_{yy}} (d_{zid} + h_0) (C_{Dsf} \bar{c}_{sf} d_{xsf} - C_{Dsr} \bar{c}_{sr} d_{xsr}) \quad (24)$$

$$M_h = \frac{\rho u_0^2}{2I_{yy}} \cdot (d_{zid} + h_0) (C_{Dsf} \bar{c}_{sf} + C_{Dsr} \bar{c}_{sr}) \quad (25)$$

$$M_{\delta_f} = \frac{-\rho u_0^2 S_{wf}}{2I_{yy}} (C_{D\alpha w} d_{z wf} - C_{L\alpha w} d_{x sf}) \quad (26)$$

$$M_{\delta_r} = \frac{-\rho u_0^2 S_{wr}}{2I_{yy}} (C_{D\alpha w} d_{z wr} + C_{L\alpha w} d_{x sr}) \quad (27)$$

$$Z_{\delta_f} = \frac{-\rho u_0^2 S_{wf}}{2m} C_{L\alpha w} \quad (28)$$

$$Z_{\delta_r} = \frac{-\rho u_0^2 S_{wr}}{2m} C_{L\alpha w} \quad (29)$$

The controllability matrix

$$\mathcal{C} = [\mathbf{B}_{long}, \mathbf{A}_{long} \mathbf{B}_{long}, \mathbf{A}_{long}^2 \mathbf{B}_{long}, \mathbf{A}_{long}^3 \mathbf{B}_{long}] \quad (30)$$

is of full rank, which means that the system is controllable. However, the model is unstable, as one of the eigenvalues of the longitudinal state matrix \mathbf{A}_{long} —the poles of longitudinal model—lies in the right half of the complex plane. This means that feedback control is necessary.

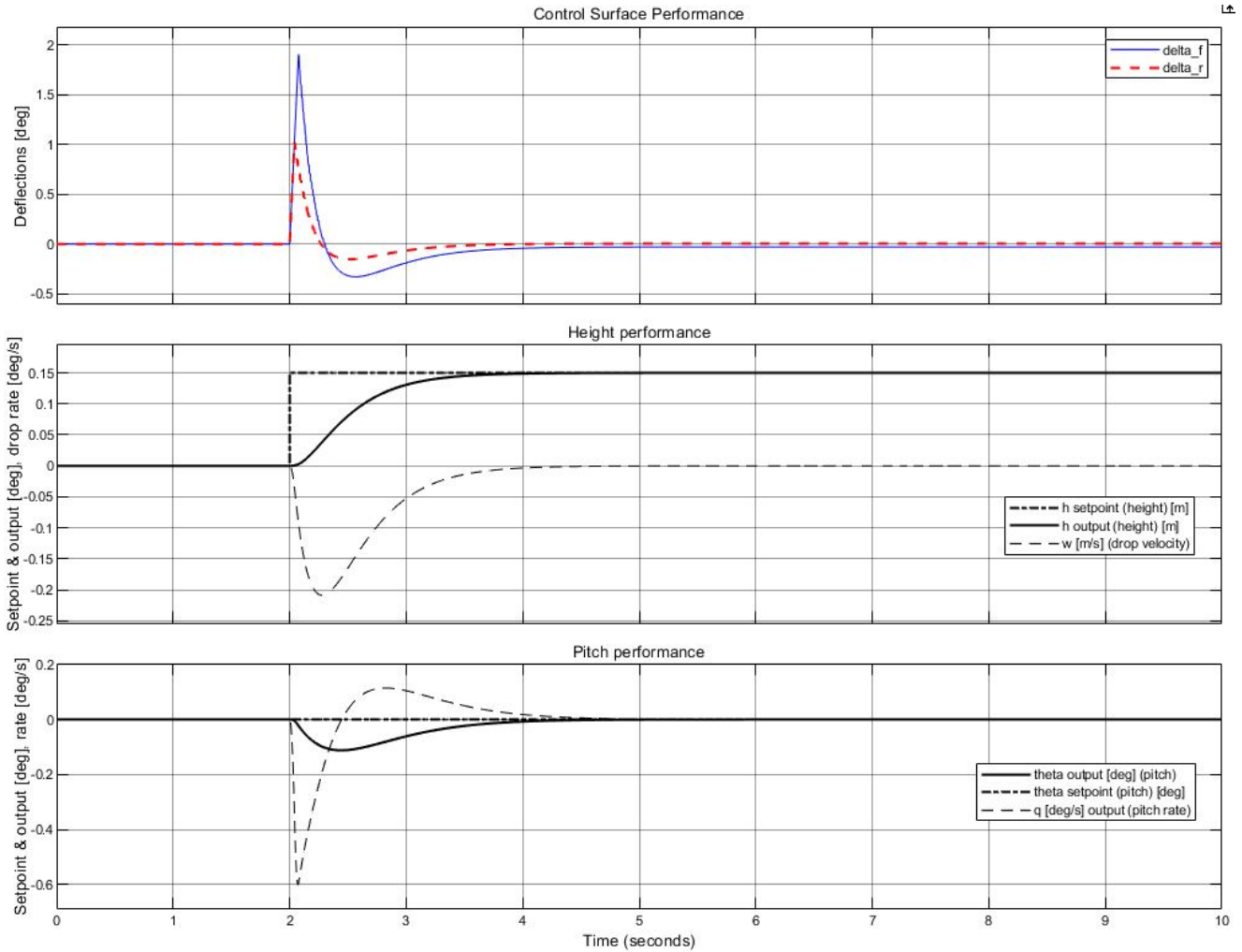


Fig. 8: The feedback controlled longitudinal model predicts good height and pitch performance during and after takeoff.

The parameters of interest are height and pitch, so

$$\mathbf{C}_{\text{place}} = \begin{bmatrix} 1 & 0 & 0 & 0 \\ 0 & 0 & 1 & 0 \end{bmatrix} \quad (31)$$

Locating the poles at -2.9 , -3.1 , -5 and -6 using the `place()` command gave satisfactory performance. The compensation matrix K_{long} has dimensions 2×4 , and the precompensation matrix has dimensions 2×2 .

As in the lateral model, the physical limitations of the boat are represented using saturation and rate limiting blocks. The front foil is limited to $+13/-6^\circ$ and $\pm 25/\text{degree/s}$, while each rear foil and therefore the rear mean angle of attack is limited to $+10/-3^\circ$ and $\pm 25^\circ/\text{s}$.

3.3 Testing and Evaluation

We then tested the stabilized system using MATLAB and Simulink like we did for the lateral model. We anticipate using a constant height setpoint once in steady level flight (after tuning the flight height for minimal drag). Therefore we passed the simulation a pitch setpoint of 0° and a step input of 0.15 m to the height setpoint to simulate takeoff.

The anticipated height and pitch performance are shown in Fig. 8. At $t = 2$ s the height setpoint steps from 0 m to 0.15 m. In response, the front and rear foils deflect upward to raise the center of gravity. The pitch only deviates by 0.1° from level flight during takeoff. Both height and pitch converge to this large step in two seconds, slow enough to act as a low-pass filter against noise as desired but fast enough to maintain steady flight. One other point of note: because this is a linear time-invariant model the speed used is the design speed of 10 m/s. However, the pre-takeoff speed

will only be about 6 m/s due to the additional drag, so the foils must deflect more to generate the lift required. Time-variant state-space theory or a model that switches between pre-takeoff and flight parameters is required to more accurately predict this transient behavior.

In addition, the pole placement may be altered to tune this behavior as shown necessary by testing on the water.

4 HARDWARE IMPLEMENTATION OF LATERAL AND LONGITUDINAL MODELS

The end goal and motivation for the development of these models is to create a working flight control system. Breaking the three-dimensional dynamics into the lateral and longitudinal components is useful, but the two models must be combined to work together.

We developed a Simulink model to read the data from the sensors, process the data into the form required by the flight control algorithm to calculate the optimal positions of the foils, then send commands to the actuators to move the control surfaces. We plan to deploy this Simulink model to a Raspberry Pi computer.

Sensors will communicate with the Raspberry Pi over a CAN (Controller Area Network) bus. Our IMU and GPS have the capability to directly interface with the CAN bus, but the ultrasonic height sensors output their values as analog voltages or as serial communication. We use custom CAN Adapters designed by previous members of the Cedarville University Solar Boat team to send and receive these values on the CAN bus.

Processing the sensor data involves interpolating the height of the center of gravity from the heights measured by the three height sensors, and differentiating this value to obtain the drop velocity. The IMU can directly provide orientation and angular velocity.

The one remaining variable is sideslip. This can theoretically be calculated through integrating the acceleration from the IMU, but in practice measurement errors accumulate leading to inaccuracy. For front & rear steering and fully combined steering, we may be able to assume that the sideslip is zero without significant loss of accuracy. We tested this with our simulation using the same yaw command as previously (Fig. 5) using the maximum yaw rates shown in Fig. 6. For the front & rear steering and fully combined models this had very little effect. More testing should be done to determine whether this is true for a variety of inputs that the boat would encounter. For the front steering and rear steering models, the models went unstable with

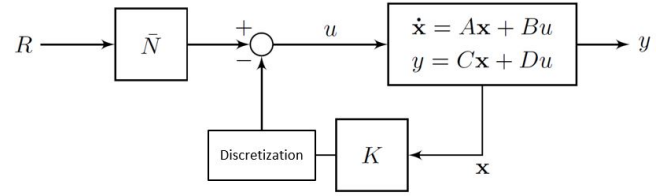


Fig. 9: Adding a discretization block represents the effect of the control system update rate.

this assumption. If a more accurate estimate of yaw rate is needed, we may require a state-space observer, such as a Kalman filter.

After using the compensation and precompensation matrices to find the required control inputs, we superimposed the mean deflection required by the longitudinal model and the differential command required by the lateral model to obtain the deflection commands for each rear foil. Because positive differential deflection must create a positive roll, the right foil must deflect downward and the left upward:

$$\delta_{rR} = \delta_r - \delta_a \quad (32)$$

$$\delta_{rL} = \delta_r + \delta_a \quad (33)$$

These must be converted to position commands for the linear actuators we are using to control the angles of attack of each control surface. The actuators are controlled using a PWM signal sent from our CAN Adapters. Our Simulink model sends a number from 0 to 255 over the CAN bus to represent the position as a proportion of the full actuator stroke. To convert the angle to this representation, we used linear interpolation between the maximum and minimum angle of our struts, valid because our struts only rotate through small angles and the actuated steering mechanisms are also nearly linear.

One major difference between our Simulink simulation and what we plan to implement on the boat is that the sensor values and actuation commands are only read at discrete time intervals. To investigate the affects this would have on the stability of the system, we added a discretization block to the compensated state vector to represent the effect of sample rate, as shown in Fig. 9. The results of this are shown in Table 1. The infinite update rate represents the performance without the time sampling block.

From these results, it appears that an update rate of 50 Hz or higher is needed to achieve close to the maximum turn rate with this model. Similar testing for the longitudinal model indicates that a sensor update

Table 1: Decreasing the lateral model sensor update frequency reduces steering performance.

Sensor Rate (Hz)	Maximum Yaw Rate ($^{\circ}/s$)
10	Unstable
20	27.65
50	28.25
100	28.40
∞	28.50

rate of 10 Hz is sufficient.

While we have tested parts of this program, we have not yet tested the whole Simulink model with a working boat. We have determined which sensors and actuators to use, where to put them, and how to wire them, but have yet to install them on the boat.

5 CONCLUSIONS & RECOMMENDATIONS

5.1 Conclusions

In this paper, we extended an existing state-space feedback model for steering control of a single-track hydrofoil boat to accurately reflect the parameters of our boat. We then used this model as a design tool to choose an appropriate combination of actuated steering inputs to obtain optimal turn performance. We also derived a feedback control model to maintain steady level flight via height and pitch control and combined the two components to function as a single flight control system for the Cedarville University Solar Boat.

We simulated the expected performance of our boat, thereby demonstrating the feasibility of using the two models in a combined automatic flight control system. We believe that this will enable the Cedarville University Solar Boat team to achieve hydrofoil flight, reducing drag and increasing race speed sufficiently to merit a return to compete at Solar Sport One.

5.2 Recommendations

Much of the software for the flight control system is nearly complete—that is, ready for testing on the boat to expose areas which require more work. We recommend that future teams emphasize installing the hardware and electronics to enable on-board testing. This may prove that several of the simplifying assumptions should be revisited and time-variant state-space theory used if needed.

We also recommended that future teams investigate

a better way to calculate or measure sideslip for the lateral model, as it is too small for our GPS to measure accurately. One potential method to better calculate sideslip is to use a Kalman filter with our boat dynamic model and the acceleration. A Kalman filter could also potentially be used to calculate more accurate horizontal and vertical velocities by combining the GPS and height sensor measurements with the acceleration measured by the IMU.

ACKNOWLEDGEMENTS

We never would have done this work without the input and guidance of our faculty advisors, Dr. Timothy Dewhurst and Dr. Gerald Brown. Thank you for your wisdom and encouragement, your willingness to talk through challenges, and your patience in pointing confused students in the right direction.

Thanks also to all our other professors who introduced us to many topics and contributed to our education and growth.

We would be remiss if we failed to thank Jason Paulus for the documentation he left to help us continue the pursuit of hydrofoil flight for the Cedarville Solar Boat.

We also extend our thanks to our families who have supported us and built us up through the years. In particular, we both wish to thank our parents for cultivating a love of learning through many hours of homeschooling that prepared us well for success at Cedarville and beyond. Thank you also for modelling excellent character, teaching wisdom by example, and pointing us to the Lord, the only true source of wisdom.

Thanks to the team-members, hallmates, friends, and classmates who have encouraged us along the way and often listened as we discussed this project even when you may not have understood any of it.

BIOGRAPHY

Ethan Beachy is a manufacturing engineer at C.F. Roark Welding and Engineering Co. in Brownsburg, IN. He earned his bachelor’s degree in Mechanical Engineering from Cedarville University, where he graduated in 2022 with highest honor. He was responsible for developing a hydrofoil flight control system for the 2022 Cedarville University Solar Boat Team as his senior design project. He is often heard singing or whistling and enjoys reading, playing disc golf and ultimate, spending time with family and friends, and participating in his church.

Jonathan Stanhope was a participant on Cedarville University's 2022 solar boat team, where he was responsible for the data acquisition system. He graduated with highest honor from Cedarville University in 2022 with a Bachelor of Science in Mechanical Engineering and currently works as a Software Engineer at Trimble in Huber Heights, OH.

References

- [1] Paulus, J. M., 2022. "A multi-input multi-output control model for a hydrofoil boat with differential front & rear strut steering and actuated-wing-induced roll". *Naval Engineers Journal*, **134**(1), pp. 33–47.
- [2] van Marrewijk, G. P., Schonebaum, J. K., and Schwab, A., 2018. "An experimentally validated dynamical model of a single-track hydrofoil boat". *Naval Engineers Journal*, **130**(1), pp. 113–134.

APPENDIX A: MODIFICATION OF LATERAL MODEL FOR STRUT VARIANCE

In his derivation of the lateral model, Paulus [1] followed the lead of TU Delft [2] in using the same linearized lift coefficient and length for each strut. However, the struts in the CU Solar Boat are not the same length and have different profiles and therefore different linearized lift coefficients. This means that some simplifications & factoring in the partial derivatives are not applicable.

Paulus presented his model as

$$\mathbf{A} = \begin{bmatrix} Y_v/m & Y_\phi/m & Y_p/m & Y_r/m - V \\ 0 & 0 & 1 & 0 \\ L_v K_{zz} + N_v K_{xz} & 0 & L_p K_{zz} + N_p K_{xz} & L_r K_{zz} + N_r K_{xz} \\ L_v K_{xz} + N_v K_{xx} & 0 & L_p K_{xz} + N_p K_{xx} & L_r K_{xz} + N_r K_{xx} \end{bmatrix} \quad (34)$$

and

$$\mathbf{B} = \begin{bmatrix} Y_{\gamma_f}/m & Y_{\gamma_r}/m & 0 \\ 0 & 0 & 0 \\ L_{\gamma_f} K_{zz} + N_{\gamma_f} K_{xz} & L_{\gamma_r} K_{zz} + N_{\gamma_r} K_{xz} & L_{\delta_a} K_{zz} + N_{\delta_a} K_{xz} \\ L_{\gamma_f} K_{xz} + N_{\gamma_f} K_{xx} & L_{\gamma_r} K_{xz} + N_{\gamma_r} K_{xx} & L_{\delta_a} K_{xz} + N_{\delta_a} K_{xx} \end{bmatrix} \quad (35)$$

We updated the appropriate terms to use the front and rear strut lift coefficient slopes and the distances from the mass center to the strut ends. The model is still subject to the assumptions presented by Paulus.

$$Y_v = -\frac{1}{2}\rho u_0 (C_{Lasf} \cdot \bar{c}_{sf} (d_{zwf} - d_{zid} - h_0) + C_{Lasr} \cdot \bar{c}_{sr} (d_{zwr} - d_{zid} - h_0)) \quad (36)$$

$$L_v = \frac{1}{4}\rho u_0 ((d_{zwf}^2 - (h_0 + d_{zid})^2) \cdot C_{Lasf} \bar{c}_{sf} + (d_{zwr}^2 - (h_0 + d_{zid})^2) \cdot C_{Lasr} \cdot \bar{c}_{sr}) \quad (37)$$

$$N_v = -\frac{1}{2}\rho u_0 \cdot (\bar{c}_{sf} (d_{zwf} - d_{zid} - h_0) \cdot d_{xsf} C_{Lasf} - \bar{c}_{sr} (d_{zwr} - d_{zid} - h_0) \cdot d_{xsr} C_{Lasr}) \quad (38)$$

$$Y_\phi = m \cdot g \quad (39)$$

$$Y_p = \frac{1}{4}\rho u_0 \cdot (C_{Lasf} \bar{c}_{sf} (d_{zwf}^2 - (h_0 + d_{zid})^2) + C_{Lasr} \bar{c}_{sr} (d_{zwr}^2 - (h_0 + d_{zid})^2)) \quad (40)$$

$$L_p = -\frac{1}{2}\rho \cdot u_0 \cdot \left(\frac{C_{L\alpha w}}{16} (S_{wf} b_{wf}^2 - S_{wr} b_{wr}^2) + \frac{C_{L\alpha sf} \bar{c}_{sf} (d_{zwf}^3 + (h_0 + d_{zid})^3)}{3} + \frac{C_{L\alpha sr} \bar{c}_{sr} (d_{zwr}^3 + (h_0 + d_{zid})^3)}{3} \right) \quad (41)$$

$$N_p = \frac{1}{4}\rho \cdot u_0 \cdot (\bar{c}_{sf} d_{xsf} C_{Lasf} (d_{zwf}^2 - (h_0 + d_{zid})^2) - \bar{c}_{sr} d_{xsr} C_{Lasr} \cdot (d_{zwr}^2 - (h_0 + d_{zid})^2)) - \frac{m \cdot g}{16 \cdot u_0} (L_{nomwf} b_{wf}^2 + L_{nomwr} b_{wr}^2) \quad (42)$$

$$Y_r = \frac{1}{2}\rho u_0 \cdot (-\bar{c}_{sf} d_{xsf} C_{Lasf} \cdot (d_{zwf} - d_{zid} - h_0) + \bar{c}_{sr} d_{xsr} C_{Lasr} (d_{zwr} - d_{zid} - h_0)) \quad (43)$$

$$L_r = \frac{1}{4}\rho u_0 \cdot (\bar{c}_{sf} d_{xsf} C_{Lasf} \cdot (d_{zwf}^2 - (d_{zid} + h_0)^2) - \bar{c}_{sr} d_{xsr} C_{Lasr} (d_{zwr}^2 - (d_{zid} + h_0)^2) + \frac{m \cdot g}{8 \cdot u_0} (L_{nomwf} b_{wf}^2 + L_{nomwr} b_{wr}^2)) \quad (44)$$

$$Y_{\gamma_f} = \frac{1}{2}\rho u_0^2 \cdot \bar{c}_{sf} C_{Lasf} \cdot (d_{zwf} - d_{zid} - h_0) \quad (45)$$

$$L_{\gamma_f} = -\frac{1}{4}\rho u_0^2 \cdot \bar{c}_{sf} C_{Lasf} (d_{zwf}^2 + (h_0 + d_{zid})^2) \quad (46)$$

$$N_{\gamma_f} = \frac{1}{2}\rho u_0^2 \cdot \bar{c}_{sf} d_{xsf} C_{Lasf} \cdot (d_{zwf} - d_{zid} - h_0) \quad (47)$$

$$Y_{\gamma_r} = \frac{1}{2}\rho u_0^2 \cdot \bar{c}_{sr} C_{Lasr} \cdot (d_{zwr} - d_{zid} - h_0) + F_T \quad (48)$$

$$L_{\gamma_f} = -\frac{1}{4}\rho u_0^2 \cdot \bar{c}_{sr} C_{Lasr} (d_{zwr}^2 + (h_0 + d_{zid})^2) - d_{zwr} F_T \quad (49)$$

$$N_{\gamma_f} = -\frac{1}{2}\rho u_0^2 \cdot \bar{c}_{sr} d_{xsr} C_{Lasr} \cdot (d_{zwr} - d_{zid} - h_0) - d_{xsr} F_T \quad (50)$$

$$L_{\delta_a} = \frac{4\tau \rho u_0^2 S_{wr} b_{wr} C_{L\alpha w}}{3\pi I_{xx}} \quad (51)$$

$$N_{\delta_a} = \frac{4k\tau \rho u_0^2 S_{wr} b_{wr} C_{L\alpha w}^2 \alpha_0}{3\pi I_{zz}} \quad (52)$$

APPENDIX B: PARAMETER VALUES

The values for our boat that we used in our calculation and simulation are included below.

Symbol & Meaning	Value	Units
b_{wf} Front wingspan	0.3527	m
b_{wr} Rear wingspan	0.9036	m
C_{Dw0} Wing reference drag coefficient	0.0074	-
$C_{D\alpha w}$ Wing drag coefficient slope	0.2982	rad ⁻¹
C_{Dsf} Front strut drag coefficient	0.0107	-
C_{Dsr} Rear strut drag coefficient	0.017	-
C_{Lw0} Wing reference lift coefficient	0.5	-
$C_{L\alpha w}$ Wing lift coefficient slope	3.867	rad ⁻¹
C_{Ls0} Strut reference lift coefficient (both)	0.0	-
$C_{L\alpha sf}$ Front strut lift coefficient slope	5.61	rad ⁻¹
$C_{L\alpha sr}$ Rear strut lift coefficient slope	3.60	rad ⁻¹
\bar{c}_{sf} Front strut chord	0.1	m
\bar{c}_{sr} Rear strut chord	0.2	m
d_{xsf} COM to front strut COP (x)	3.365	m
d_{xsr} COM to rear strut COP (x)	0.852	m
d_{zid} Idealized waterline offset	0.02	m
d_{zwf} COM to front foil (z)	0.613	m
d_{zwr} COM to rear foil (z)	0.537	m
F_T Estimated thrust force	167	N
g Gravitational acceleration	9.81	m·s ⁻²
h_0 Design flight height	0.15	m
L_{nomwf} Nominal front lift ratio	0.2	-
L_{nomwr} Nominal rear lift ratio	0.8	-
m Boat total mass	222	kg
k Empirical aileron constant	-0.058	-
S_{wf} Front wing surface area	0.0119	m ²
S_{wr} Rear wing surface area	0.0990	m ²
u_0, V Design speed	10	m·s ⁻¹
I_{xx} X-axis moment of inertia	26.16	kg·m ²
I_{yy} Y-axis moment of inertia	584.6	kg·m ²
I_{zz} Z-axis moment of inertia	602.3	kg·m ²
I_{xz} XZ product of inertia	-14.54	kg·m ²
α_0 Wing zero-lift axis	-0.134	rad
ρ Water density	998.6	kg·m ⁻³
τ Flap efficiency factor	1	-